

Supplementary Information

Structure- and Porosity-Tunable, Thermally Reactive Metal Organic Framework for High-Performance Ni-rich Layered Oxide Cathode Materials

Jun-Ho Park,^{ae} Kwangjin Park,^b Dongwook Han,^{*cf} Dong-Hee Yeon,^a Heechul Jung,^a Byungjin Choi,^a
Seong Yong Park,^d Sung-Jin Ahn,^a Jin-Hwan Park,^a Heung Nam Han^e and Kang Hee Lee^{*a}

^a Energy Lab, Samsung Advanced Institute of Technology (SAIT), Electronic Materials Research Complex, 130 Sam-sung-ro, Gyeonggi-do, 16678, Republic of Korea.

^b Department of Mechanical Engineering, Gachon University, 1342 Seongnamdaero, Sujeong-gu, Seongnam-si, Gyeonggi-do, Republic of Korea.

^c School of Nano Convergence Technology, Hallym University, 1 Hallymdaehak-gil, Chuncheon, Gangwon-do, 24252, Republic of Korea.

^d Analytical Department, Samsung Advanced Institute of Technology (SAIT), Electronic Materials Research Complex, 130 Samsung-ro, Gyeonggi-do, 16678, Republic of Korea.

^e Department of Materials Science and Engineering and Research Institute of Advanced Materials, Seoul National University, Seoul 151-744, Republic of Korea.

^f Nano Convergence Technology Center, Hallym University, 1 Hallymdaehak-gil, Chuncheon, Gangwon-do, 24252, Republic of Korea.

List of Figures and Tables

Figure S1. Thermogravimetric analysis curve of metal-organic framework ZIF-67 up to 750 °C.

Figure S2. (a) Co 2p XPS spectra of bare, 1 wt.% MOF-treated, and 6 wt.% MOF-treated Ni-rich NCM (sputtering was not carried out). (b) Thermodynamic stability of Co-O, Ni-O, Co₃N, and Co₂C chemical bonds with temperature calculated by HSC chemistry simulation.

Figure S3. Cross-sectional high-angle annular dark field scanning transmission electron microscopy (HAADF-STEM) images and the corresponding EELS spectra (Ni, Co) of 1 wt.% MOF-treated Ni-rich NCM.

Figure S4. Pore size distributions of bare, 1 wt.% MOF-treated, and 6 wt.% MOF-treated Ni-rich NCM.

Figure S5. Microstructure of 8 wt.% of Co ions surface-treated Ni-rich NCM by a conventional wet process.

Figure S6. X-ray diffraction pattern of MOF (ZIF-67).

Figure S7. Changes in the particle morphology of Ni-rich NCM with increasing MOF content.

Figure S8. EIS data for bare, and 1 wt.% MOF-treated Ni-rich NCM after the 50th cycles.

Table S1. Inductively coupled plasma-atomic emission spectrometry (ICP-AES) results for MOF (ZIF-67).

Table S2. Results of Brunauer-Emmett-Teller (BET) analysis of N₂ adsorption–desorption isotherms for bare, 1 wt.% MOF-treated, and 6 wt.% MOF-treated Ni-rich NCM.

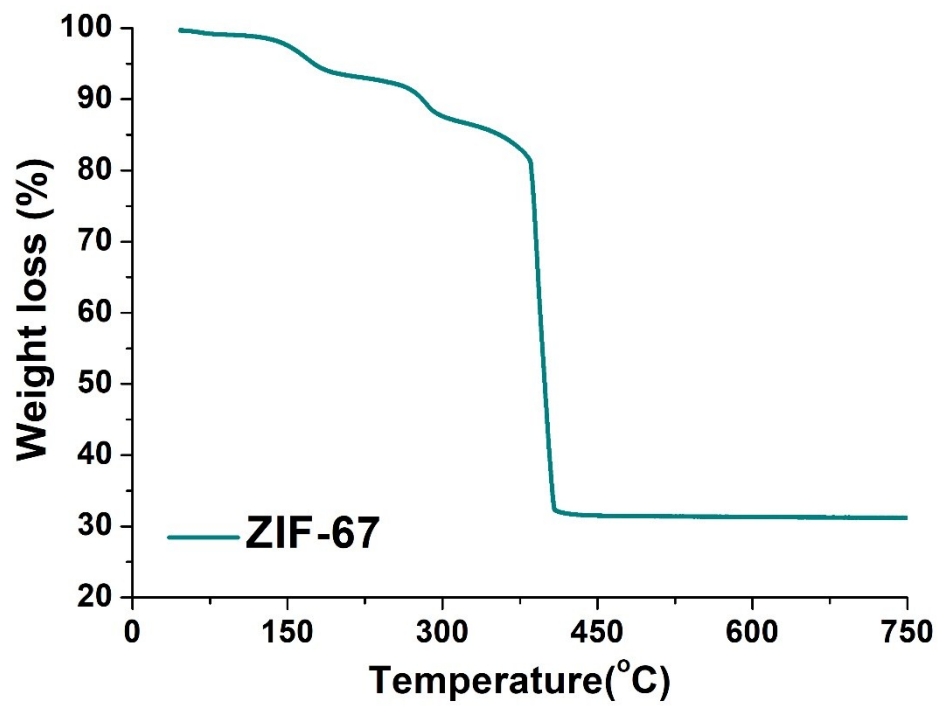


Figure S1. Thermogravimetric analysis curve of metal-organic framework ZIF-67 up to 750 °C.

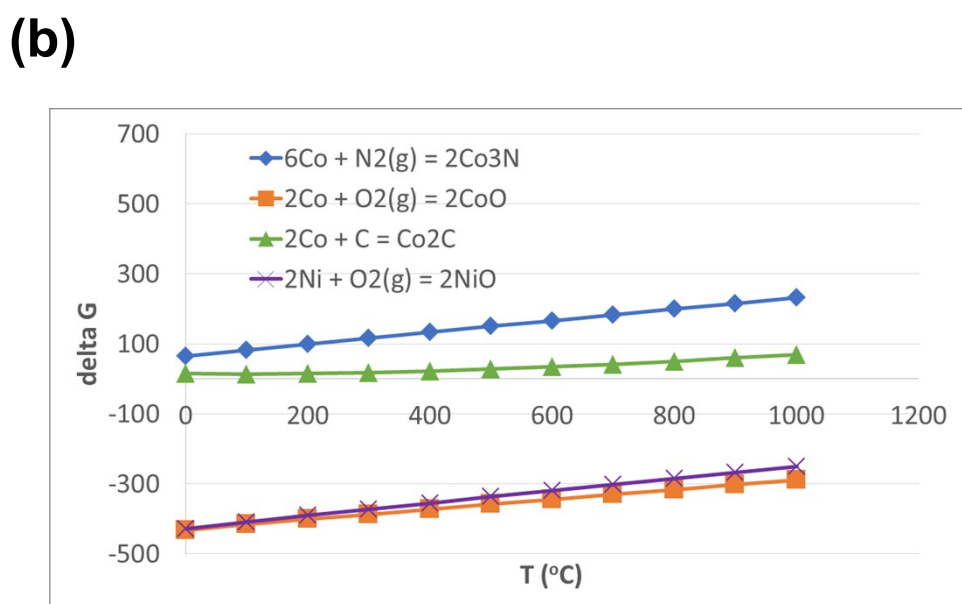
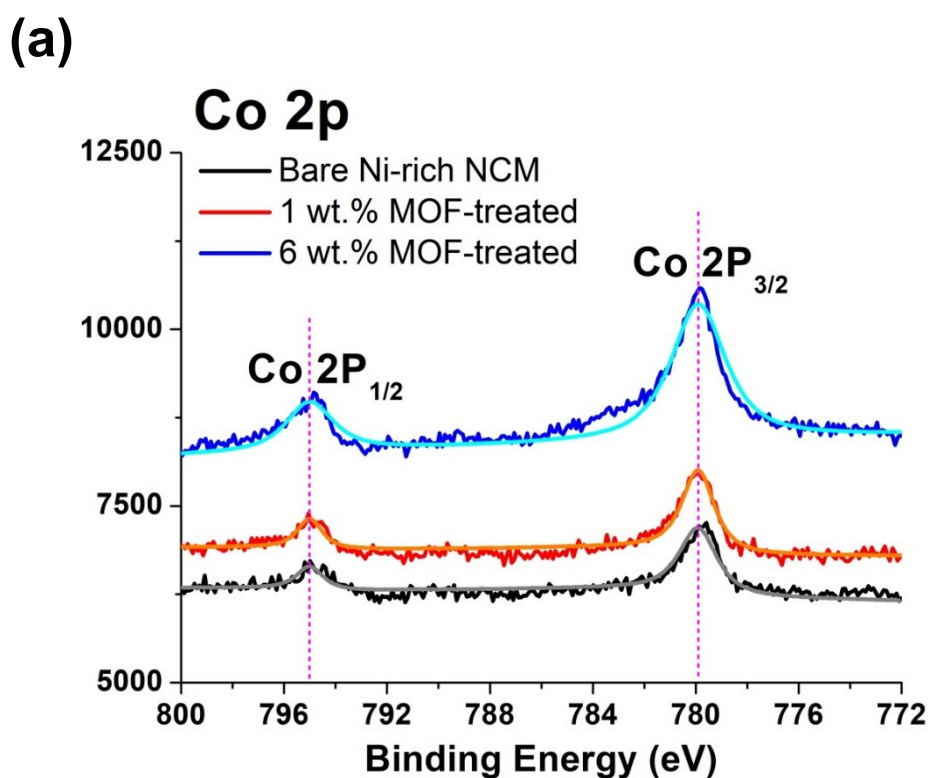


Figure S2. (a) Co 2p XPS spectra of bare, 1 wt.% MOF-treated, and 6 wt.% MOF-treated Ni-rich NCM (sputtering was not carried out). (b) Thermodynamic stability of Co-O, Ni-O, Co_3N , and Co_2C chemical bonds with temperature, simulated by using the HSC chemistry software (provided by Outokumpu Research). The HSC chemistry simulation is to calculate the equilibrium energies for chemical reactions with extensive thermochemical database including enthalpy, entropy, and Gibbs free energy.

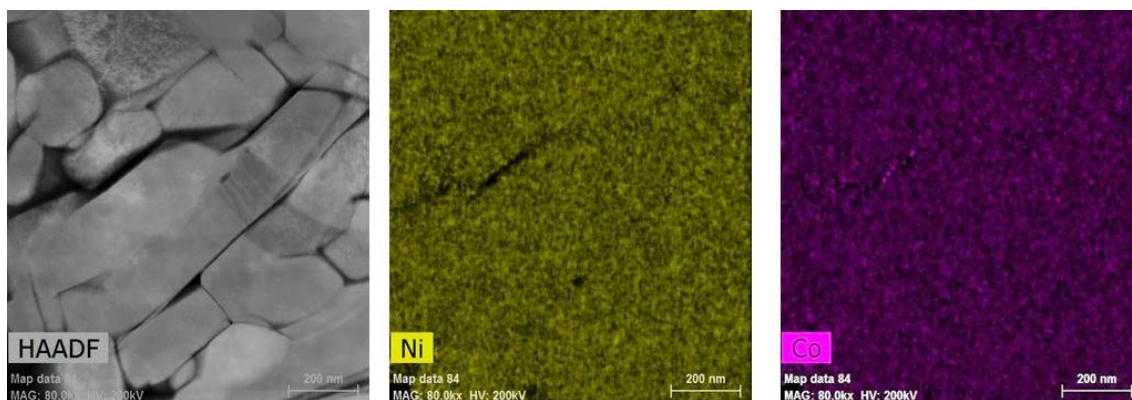


Figure S3. Cross-sectional high-angle annular dark field scanning transmission electron microscopy (HAADF-STEM) images and the corresponding EELS spectra (Ni, Co) of 1 wt.% MOF-treated Ni-rich NCM.

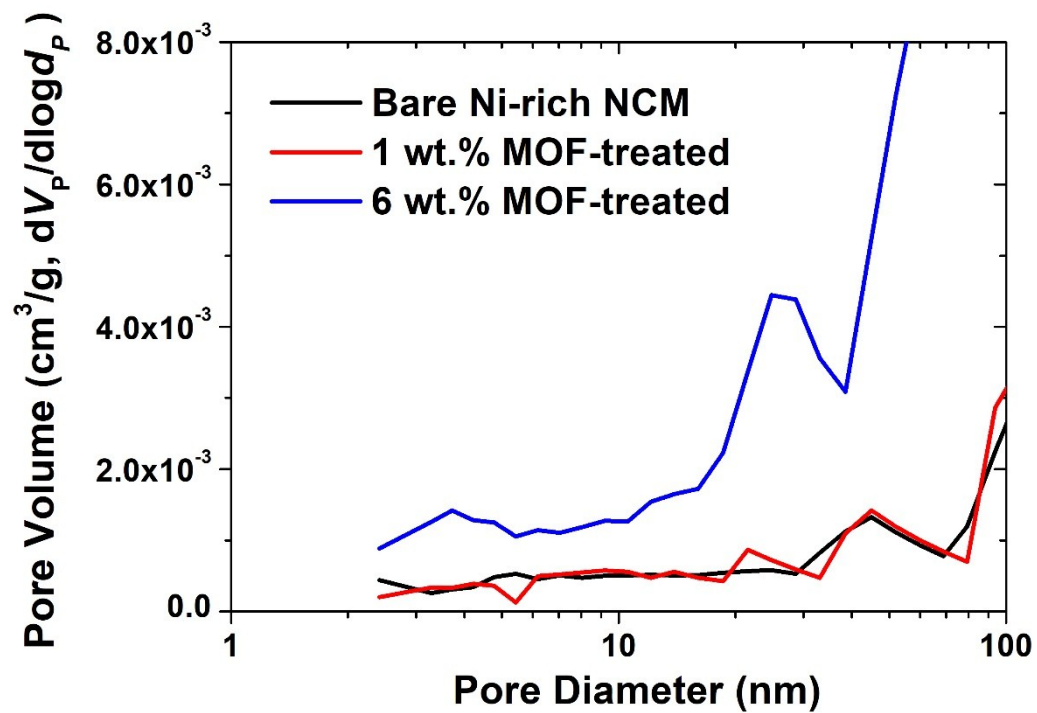


Figure S4. Pore size distributions of bare, 1 wt.% MOF-treated, and 6 wt.% MOF-treated Ni-rich NCM.

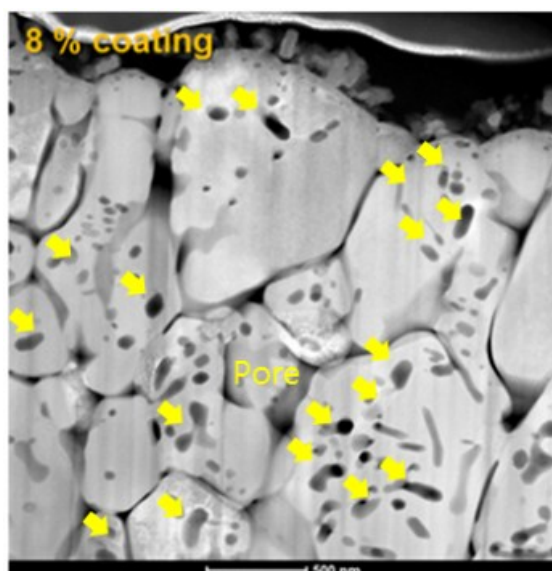


Figure S5. Microstructure of 8 wt.% of Co ions surface-treated Ni-rich NCM by a conventional wet process.

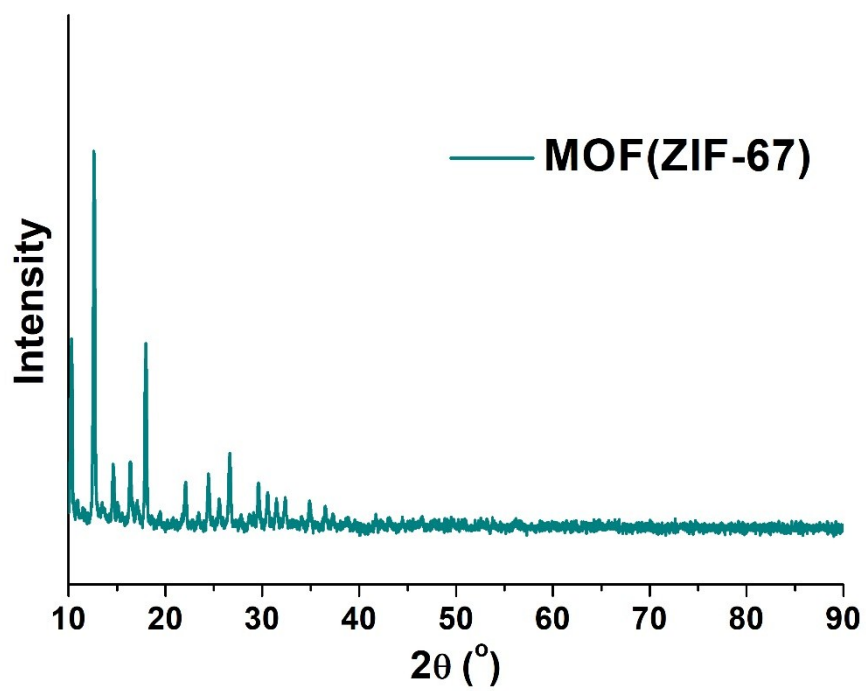


Figure S6. X-ray diffraction pattern of MOF (ZIF-67).

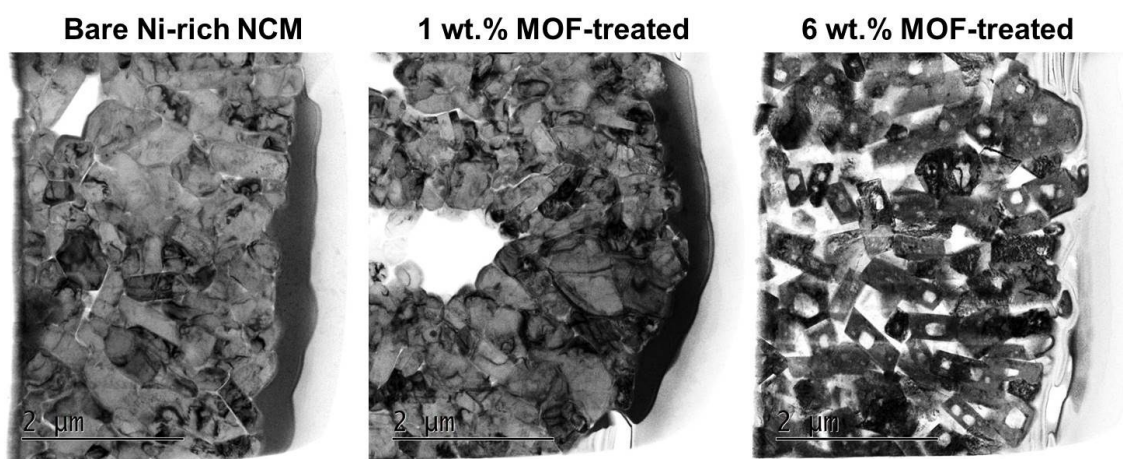


Figure S7. Changes in the particle morphology of Ni-rich NCM with increasing MOF content.

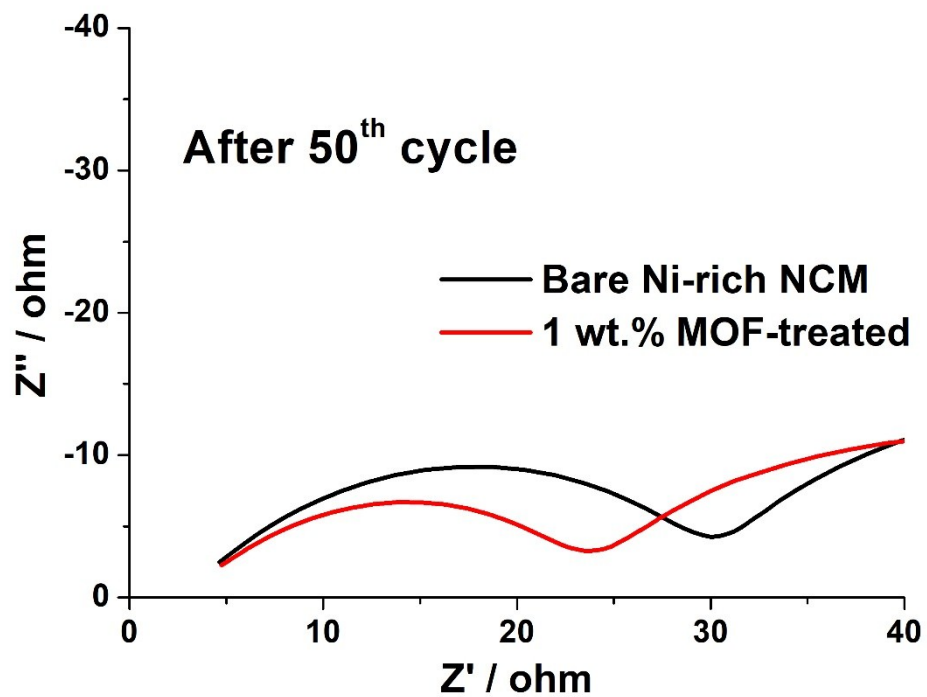


Figure S8. EIS data for bare, and 1 wt.% MOF-treated Ni-rich NCM after the 50th cycles.

Table S1. Inductively coupled plasma-atomic emission spectrometry (ICP-AES) results for MOF (ZIF-67).

Sample	ICP-AES, %w/w			
	Li	Mn	Co	Ni
ZIF-67	-	-	22.76	-

Table S2. Results of Brunauer-Emmett-Teller (BET) analysis of N₂ adsorption–desorption isotherms for bare, 1 wt.% MOF-treated, and 6 wt.% MOF-treated Ni-rich NCM.

Sample	$a_{s,BET}$ [m ² g ⁻¹]
Bare Ni-rich NCM	0.47954
1 wt.% MOF-treated	0.48603
6 wt.% MOF-treated	1.4141